Study on Frequency Tracking and Load Output Voltage Control for the LCL-type Inductive Power Transfer System

Jikun ZHOU *, Qiongdan ZHANG, Rong ZHANG
Institute of systems engineering, China academy engineering of physics, Mianyang, 621999, China

***Abstract*—In the LCL-type inductive power transfer (IPT) system, the zero current switching (ZCS) frequency of system drifts with load variation which cause high VA rating of the power supply and the load output voltage unstable. To deal with these two problems, this paper presents a dual-loop control method to realize ZCS frequency tracking and load output voltage stable when load variation. The inner loop controller uses the convertor output current phase character signal to synchronize the converter operator frequency such that the operation frequency can track the ZCS frequency. In the out loop control system, considering nonlinearity and frequency uncertainty character of system, a H∞ controller base on generalized state space averaging (GSSA) modeling method is designed for load voltage stable control. The control algorithms are embedded in FPGA and DSP respectively, and the experiment results verify the control method.**

***Index Terms*—LCL-type IPT system, H∞ control, generalized state space averaging, frequency tracking.**

I. INTRODUCTION

Inductive power Transfer (IPT) system has been used in many commercial and industrial applications [1-3]. To achieve higher power transfer and other advantages, an inductor/capacitor/inductor (LCL) resonant convertor is used in IPT applications which called LCL-type IPT system [4-6]. However, loosely coupled between primary coil and secondary coil that causes the primary ZCS frequency easily drifts with load variation, and also make the load voltage unstable [7-8]. Therefore, the frequency tracking and load output voltage control is required for LCL-type IPT system. To data, some researches has been undertake for frequency control or load voltage control. A voltage across $R_{DS(on)}$ of the power MOSFET is utilized to compensate the resonance features of IPT system to make operation frequency closely locked with the primary current phase [9]. But, this method only adapt current field IPT system, and the load output voltage stable is not considered. Load output voltage control strategies including short circuit decoupling method [10], multiple resonant point control [11] and robust control [12]. However, the research did not consider convertor operator frequency. In this paper, a dual-loop control method is presented, and the inner loop controller is used to make the operator frequency tracking the ZCS frequency of convertor while the out loop controller realizes load output voltage control.

The impedance of the secondary Zs is given by

II FREQUENCY TRACKING CONTROLLER DESIGN

A. *Frequency Uncertain Analysis*

The topology of LCL-type IPT system is show in Fig.1. The primary part is LCL resonant tank. In this paper, the parallel compensation is selected for secondary part. Where V_{in} is the output voltage of full-brig convertor.

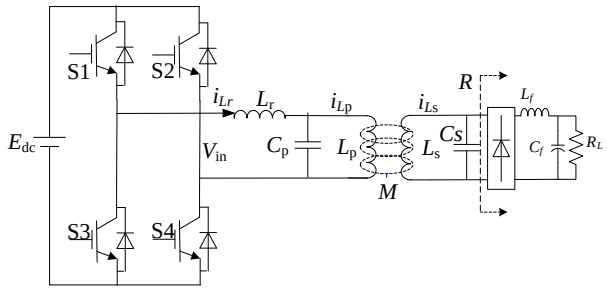

Figure.1 topology of LCL-type IPT system

The standard mutual inductance coupling model of system is shown in Fig.2.

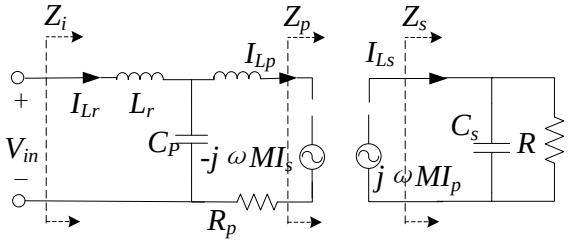

Figure.2 mutual inductance coupling model

Where R is the equal resistance of load R_L and rectifier, and can be calculated by

$$R = \frac{\pi^2}{8} R_L \tag{1}$$

$$Z_s = j\omega L_s + \frac{1}{j\omega C_s + 1/R} \tag{2}$$

The reflected impedance Z_p depended on the transformer coupling and operating frequency is given by

$$Z_p = \frac{\omega^2 M^2}{Z_s} \tag{3}$$

Then, the total impedance of the system Z_i can be calculated as

$$Z_i(\omega, R_L) = j\omega L_r + R_r + \frac{1}{j\omega C_p + 1/(j\omega L_p + R_p + \omega^2 M^2 / Z_s)} \tag{4}$$

It can be see that, the image part of the total impedance will change with the load R_L. To achieve minimum VA rating of the power supply, it is necessary to change the operating frequency ω to make the image part of the total impedance equal to zero. In other words, the operator frequency must equal to the system' zero phase angle frequency which also the ZCS frequency. In this paper a frequency track controller is designed to ensure to operator frequency tracking the zero phase angle frequency when load variation.

B. Frequency track controller design

To ensure the full bridge convertor working at the ZCS condition, the MOSFET would be conducted or closed when convertor output current i_{Lr} is zero.

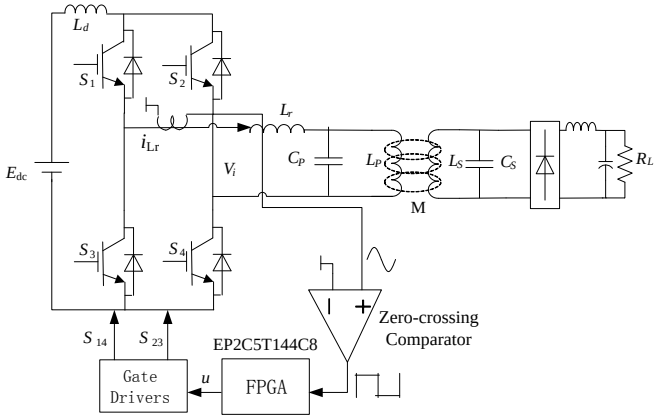

Figure.3 The structure of frequency track control system

As this ideal, the convertor output current's phase character signal can be detect and used to synchronize the converter switch. Fig.3 shows the structure of frequency tracking control system. The controller is implemented on a FPGA development kit based on the EPM2C5T144C8 chip, a zero-crossing comparator is used to transform the current's phase character signal in to digital square signal. when the current i_{Lr} is bigger than zero, the output of zero-crossing comparator is '1', other the output of zero-crossing comparator is '0'. The control signal $u(t)$ depend on the current phase character signal is given by

$$u(t) = \begin{cases} 1 & i_{Lr} > 0 \\ 0 & i_{Lr} \le 0 \end{cases} \tag{5}$$

When $u(t)=1$, the mosfet S_1 and S_4 is conducted, S_2 and S_3 is closed. When $u(t)=0$, the mosfet S_2 and S_3 is conducted, S_1 and S_4 is closed.

III. UNCERTAINTY MODELING

A. GSSA Modeling

As seen in Fig.1, the state variable of LCL-type system can be define as

$$\mathbf{X} = [i_{Lr}, i_{Lp}, u_{Cp}, i_{Ls}, u_{Cs}, i_{Lf}, u_{Cf}] \tag{6}$$

However, with primary inverter and secondary rectifier, the time domain differential equations of LCL-type system is nonlinear which make it difficult to synthesis a controller for load output voltage control. The aim of Generalized State-Space Averaging (GSSA) method is approximate the time domain variables by interval of its zero and first-order Fourier series.

Define $\langle x\rangle_0$ and $\langle x\rangle_1$ ($\langle x\rangle_{-1}$) as the zero and first-order Fourier coefficients of the circuit variables respectively. When work at the ZCS frequency, original circuit variables can be approximated calculated as the following equations:

$$\begin{cases} i_{Lr} = \langle i_{Lr}\rangle_1 e^{j\omega t} + \langle i_{Lr}\rangle_{-1} e^{-j\omega t} \\ u_{Cp} = \langle u_{Cp}\rangle_1 e^{j\omega t} + \langle u_{Cp}\rangle_{-1} e^{-j\omega t} \\ i_{Lp} = \langle i_{Lp}\rangle_1 e^{j\omega t} + \langle i_{Lp}\rangle_{-1} e^{-j\omega t} \\ i_{Ls} = \langle i_{Ls}\rangle_1 e^{j\omega t} + \langle i_{Ls}\rangle_{-1} e^{-j\omega t} \\ u_{Cs} = \langle u_{Cs}\rangle_1 e^{j\omega t} + \langle u_{Cs}\rangle_{-1} e^{-j\omega t} \\ i_{Lf} = \langle i_{Lf}\rangle_0 \quad u_{cf} = \langle u_{Cf}\rangle_0 \end{cases} \tag{7}$$

According to Kirchhoff's circuit laws and the properties of the Fourier coefficients [13], the generalized differential equations of system can be given by

$$\begin{cases} \langle i_{Lr}\rangle_1' = -L_r^{-1} R_r \langle i_{Lr}\rangle_1 - L_r^{-1}\langle u_{Cp}\rangle_1 - L_r^{-1}\langle g_1(t)u_{dc}\rangle_0 - j\omega\langle i_{Lr}\rangle_1 \\ \langle u_{Cp}\rangle_1' = C_p^{-1}\langle i_{Lr}\rangle_1 + C_p^{-1}\langle i_{Lp}\rangle_1 - j\omega\langle u_{Cp}\rangle_1 \\ \langle i_{Lp}\rangle_1' = \det^{-1}(-L_s\langle u_{Cp}\rangle_1 + L_s R_p\langle i_{Lp}\rangle_1 + MR_s\langle i_{Ls}\rangle_1 + M\langle u_{Cs}\rangle_1 \\ \qquad -\pi^{-1}2M\langle u_{cf}\rangle_0) - j\omega\langle i_{Lp}\rangle_1 \\ \langle i_{Ls}\rangle_1' = \det^{-1}(-M\langle u_{Cp}\rangle_1 + MR_p\langle i_{Lp}\rangle_1 + L_p R_s\langle i_{Ls}\rangle_1 + -1L_p\langle u_{Cs}\rangle_1 \\ \qquad +\pi^{-1}2L_p\langle u_{cf}\rangle_0 - j\omega\langle i_{Ls}\rangle_1 \\ \langle u_{cs}\rangle_1' = C_s^{-1}\langle i_s\rangle_1 - j\omega\langle V_{cs}\rangle_1 \\ \langle i_{Lf}\rangle_0' = -L_f^{-1}\langle g_2(t)u_{cs}\rangle_1 - L_f^{-1}\langle u_{cf}\rangle_0 \\ \langle u_{cf}\rangle_0' = -C_f^{-1}\langle g_2(t)i_{Ls}\rangle_1 - C_f^{-1}R_L^{-1}\langle u_{cf}\rangle_0 \end{cases} \tag{8}$$

Where **det**=M^2-L_pL_s and $g_1(t)$ and $g_2(t)$ stand for the primary and secondary switch functions respectively. Separating the real and imaginary parts of (8), the GSSA variables can be given by.

$$\begin{aligned}\mathbf{X}_{gssa}(\mathbf{t}) = [&\mathrm{Re}\langle i_{Lr}\rangle_1, \mathrm{Im}\langle i_{Lr}\rangle_1, \mathrm{Re}\langle u_{Cp}\rangle_1, \mathrm{Im}\langle u_{Cp}\rangle_1 \\ &\mathrm{Re}\langle i_{Lp}\rangle_1, \mathrm{Im}\langle i_{Lp}\rangle_1, \mathrm{Re}\langle i_{Ls}\rangle_1, \mathrm{Im}\langle i_{Ls}\rangle_1 \\ &\mathrm{Re}\langle u_{Cs}\rangle_1, \mathrm{Im}\langle u_{Cs}\rangle_1, \langle i_{Lf}\rangle_0 \langle u_{Cf}\rangle_0]^T\end{aligned} \quad (9)$$

With GSSA variables, the GSSA differential model is given by

$$\dot{\mathbf{X}}_{gssa} = \mathbf{A}\mathbf{X}_{gssa} + \mathbf{B}u \quad (10)$$

Where A and B as the constant matrices denote the system matrix and control matrix respectively, and the GSSA model is a linear model in frequency domain.

B. Ltfs For GSSA Model

Considering the zero phase angle drift with load variation, uncertainty modeling proceeds with regard to the load and frequency uncertainty with its value within certain know interval, and are given by

$$\omega = \bar{\omega}(1 + p_\omega \delta_\omega), R_L = \bar{R}_L(1 + p_r \delta_r) \quad (11)$$

Where $\bar{\omega}$ and $\bar{R}_L$ are the nominal value of ω and R respectively. $p_\omega\delta_\omega$ and $p_r\delta_r$ stand for the relative perturbation on frequency and laod, which satisfies the norm condition $\|\delta_\omega\| \le 1$ and $\|\delta_r\| \le 1$.

For instants, p_ω=0.2 represents 20% uncertainty in the frequency. ω and R_L can be represented as an upper LFT in δ_ω and δ_r respectively .The LFT about ω and R_L can be depicted by the block diagram in Fig.4. Where $y_{i\omega}$, y_{jr} and $v_{i\omega}$, v_{jr} stand for the input and ouput of δ_ω and δ_r respectively, x_i and x_j denote one of the system sate variables.

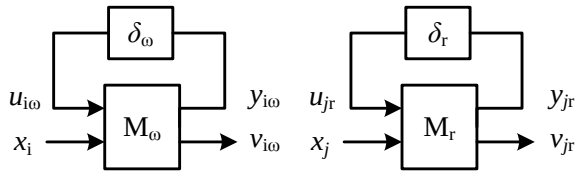

Figure.4 Linear fractional transformation for uncertain parameters ω and RL

The relationship between input and output of $\mathbf{M}_\omega$ and $\mathbf{M}_r$ can be given by

$$\begin{bmatrix} y_{i\omega} \\ v_{i\omega} \end{bmatrix} = \begin{bmatrix} 0 & \bar{\omega} \\ \delta_\omega & \bar{\omega} \end{bmatrix} \begin{bmatrix} u_{i\omega} \\ x_i \end{bmatrix} = \begin{bmatrix} \bar{\omega} x_i \\ \delta_\omega u_{i\omega} + \bar{\omega} x_i \end{bmatrix} \quad (12)$$

$$\begin{bmatrix} y_{jr} \\ v_{jr} \end{bmatrix} = \begin{bmatrix} -\delta_r & 1/\bar{R}_L \\ -\delta_r & 1/\bar{R}_L \end{bmatrix} \begin{bmatrix} u_{jr} \\ x_j \end{bmatrix} = \begin{bmatrix} -\delta_r u_{jr} + x_j/\bar{R}_L \\ -\delta_r u_{jr} + x_j/\bar{R}_L \end{bmatrix} \quad (13)$$

Then, the uncertain parameter δ_ω and δ_r are separated from (11), which can be presented as a uncertain matrix

$$\mathbf{\Delta} = diag\{\delta_\omega, \cdots, \delta_\omega, \delta_r\} \quad (14)$$

Where $\mathbf{\Delta} \in \mathbf{C}^{12\times 12}$ is an unknown diagonal matrix and satisfies the norm condition $\|\mathbf{\Delta}\|_\infty \le 1$.

The input and output of uncertain matrix are given by

$$\mathbf{w} = pertin = [y_{1\omega}, y_{2\omega}, \cdots, y_{9\omega}, y_{10r}]^T \quad (15)$$

$$\mathbf{p} = perout = [u_{1\omega}, u_{2\omega}, \cdots, u_{9\omega}, u_{10r}]^T \quad (16)$$

Though LFT operator, the uncertainty parts is separated from systems GSSA model as show in fig.5. Where the remind part G_{mds} is the nominal mode, the input vector $\boldsymbol{u}$ includes reference signals, noises and external disturbances.

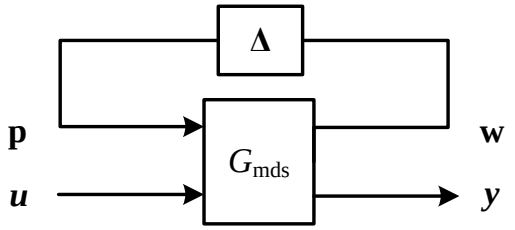

Figure.5 Unknown model of system

The GSSA model of LCL IPT system can be transformed to a linear system with perturbation feedback.

$$\begin{cases} \dot{\mathbf{x}} = \mathbf{A}\mathbf{x} + \mathbf{B_1}\mathbf{p} + \mathbf{B_2}\mathbf{u} \\ \mathbf{w} = \mathbf{C_1}\mathbf{x} + \mathbf{D_{11}}\mathbf{p} + \mathbf{D_{12}}\mathbf{u} \\ \mathbf{y} = \mathbf{C_2}\mathbf{x} + \mathbf{D_{21}}\mathbf{p} + \mathbf{D_{22}}\mathbf{u} \end{cases} \quad (17)$$

As for (16), **x** stand for the state variable of GSSA model, **y** is the system output voltage, vector **p** and **w** stand for the uncertainty extern al signals.

IV. DESIGN OF THE H∞ CONTROLLER

For the uncertain model of LCL type IPT system, to realize robust control for load output voltage under load and frequency, a H∞ controller u(s)=K(s)y(s) base on mixed sensitivity is design and the structure of control system is show as fig.6.

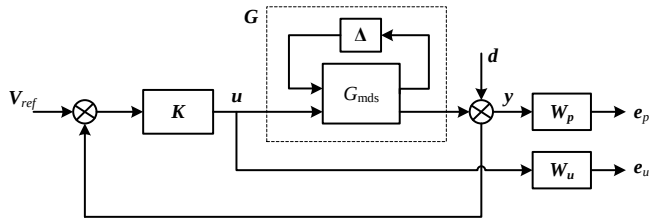

Fig.6 Output feedback H∞ control scheme with mixed sensitivity

Where, V_{ref} is the reference input voltage, and $\mathbf{G}=F_u(\boldsymbol{G}_{mds}, \boldsymbol{\Delta})$ is the perturbation feedback model of LCL type IPT system, $\boldsymbol{d}$ is a disturbance on load output voltage and $\boldsymbol{d}\in\boldsymbol{L}_2$; $\boldsymbol{W}_p$ and $\boldsymbol{W}_u$ are weighted functions. The control system can be transformed to a standard feedback control system structure as show in fig.7.

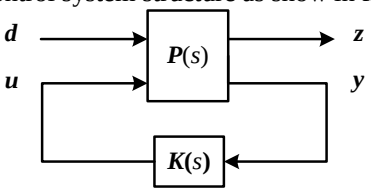

Fig.7 Stander structure of feedback control

Where, d is external disturbance, and z=[ep,eu]T is performance index function is load output voltage is control signal(s) is LCL type IPT system model. The aim of design the controller is find a feedback controller K(s), which makes the system stability and the H∞ norm of feedback transfer function Tdz(s) from d to z below an index (γ>0), which can be given by

$$\left\| \begin{matrix} W_p(\mathbf{I}+\mathbf{GK})^{-1} \\ W_u\mathbf{K}(\mathbf{I}+\mathbf{GK})^{-1} \end{matrix} \right\|_\infty < \gamma \text{ or } \left\|\mathbf{F}_L(\mathbf{P},\mathbf{K})\right\|_\infty < \gamma \qquad (18)$$

The H_∞ controller can be given by

$$\mathbf{K}(s)=\begin{bmatrix} \mathbf{A}_f & -\mathbf{ZL} \\ \mathbf{F} & 0 \end{bmatrix} \qquad (19)$$

Where $\mathbf{A}_f=\mathbf{A}+\gamma^{-2}\mathbf{B}_1\mathbf{B}_1{}^T\mathbf{X}+\mathbf{B}_2\mathbf{F}+\mathbf{ZLC}_2$, $\mathbf{Z}=(\mathbf{I}-\gamma^{-2}\mathbf{YX})^{-1}$, $\mathbf{F}=-\mathbf{B}_2{}^T\mathbf{X}$. $\mathbf{X}$ and $\mathbf{Y}$ can be acquired by solving two algebra Riccati function given by

$$\begin{cases} \mathbf{A}^T\mathbf{X}+\mathbf{XA}+\mathbf{X}(\gamma^{-2}\mathbf{B}_1\mathbf{B}_1{}^T-\mathbf{B}_2\mathbf{B}_2{}^T)X+\mathbf{C}_1\mathbf{C}_1{}^T=0 \\ \mathbf{AY}+\mathbf{YA}^{\mathbf{T}}+\mathbf{Y}(\gamma^{-2}\mathbf{C}_1{}^{\mathbf{T}}\mathbf{C}_1-\mathbf{C}_2{}^{\mathbf{T}}\mathbf{C}_2)\mathbf{Y}+\mathbf{B}_1{}^{\mathbf{T}}\mathbf{B}_1=0 \end{cases} \qquad (20)$$

V. EXPERIMENTAL RESULTS

The experiment system for LCL-type IPT system is established to verify the dual-loop control method as showed in Fig.10. In the out loop control system, the H∞ controller is implemented on a DSP development kit based on the DSP2812 chip, load output voltage U_f is sampled and sent to the controller (DSP) by RF transmitter while the reference voltage is given by PC though RS232 bus. Then, the controller regulates the input voltage E_{dc} to make the output voltage to equal the reference voltage with a buck converter.

The circuit parameters values of experiment system are listed in Table.1.

TABLE I

EXPERIMENT PARAMETER VALUES

Parameter	*Values*
Primary resonant inductance L_r (μH)	220
Primary resonant inductance L_p (μH)	110
Secondary resonant inductance L_s (μH)	110
Mutual inductance M (μH)	33
Secondary resonant capacitance C_s (μF)	0.25
Load R_L (Ω)	25, 50
Primary resonant capacitance C_p (μF)	0.374
Input voltage E_{dc} (V)	30
Filter inductance L_f (mH)	1.0
Filter inductance C_f (μF)	47

The reference voltage is set as 48V, and the load changing between 20Ω and 50Ω.

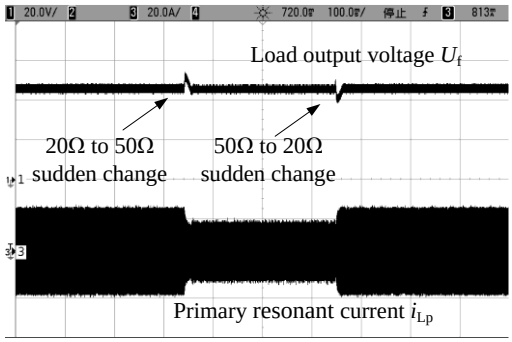

Fig.8 Experimental waveform of load variation
(Ch1: load output voltage-20V/div, Ch2: priamry current iLp-20A/div)

Fig.8 shows the load output voltage control performance under sudden load changes. Observation of Fig.9 reveals that the out loop controller can maintain the load voltage at 48V in 20ms when load variation.

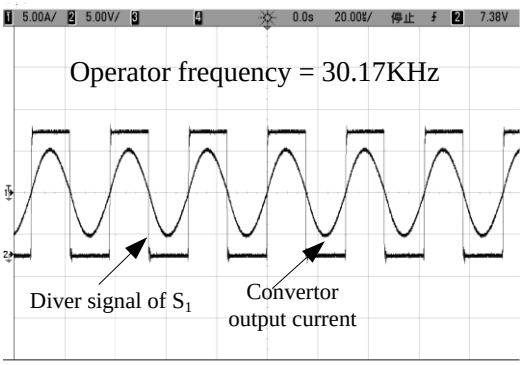

(a) R_L is 50Ω

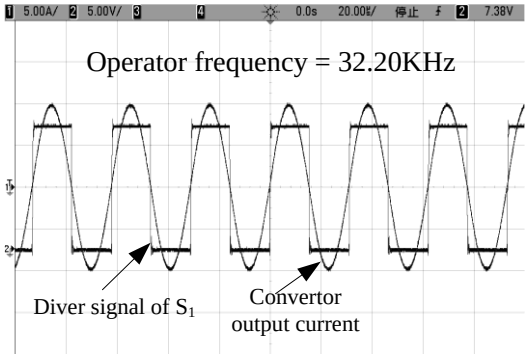

(b) R_L is 20Ω

Figure.9 steady-state waveforms with different load
(Ch1: diver voltage S1-5V/div, Ch2: convertor output current iLr-5A/div).

Fig.9 shows the measured waveforms of gate diver signal $S_{1,4}$ and convertor output current i_{Lr} with different load. As shown in Fig.10, with frequency tracking control, the operator frequency is moved from 30.17 KHz to 32.20 KHz, and the zero current switching is achieved, which validates the proposed frequency tracking control approach.

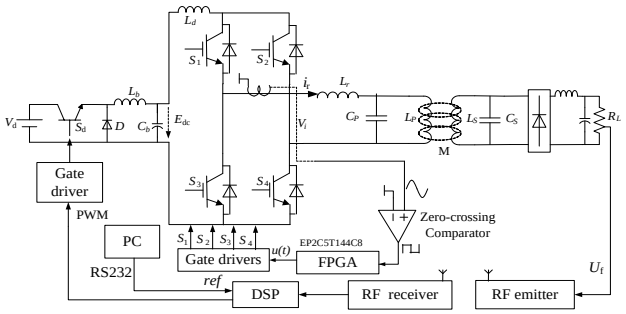

Figure.10 Experiment system structure

VI. CONCLUSION

Aimed at frequency tracking and load output voltage control of LCL-type IPT system, a dual-loop control method is proposed in this paper. In the inner loop, the controller detect current phase character signal to realize ZCS frequency tracking when load variation. At the out loop, to deal with the nonlinear and frequency drift characteristics of system, the generalized state space averaging modeling method is used to describe the system in frequency domain, and base the GSSA model, a H∞ control method is proposed to realize output voltage control. The control algorithms are embedded in FPGA and DSP respectively. The experiment results were also liven to verify the dual-loop control method."

REFERENCES

[1] O. H. Stielau, G. A. Covic. "Design of Loosely Coupled Inductive Power Transfer System," IEEE International Conference on Power System Technology, 2002, p. 85-90.

[2] Wang C, Stielau OH, Covic GA. "Design considerations for a contactless electric vehicle battery charger," IEEE Transactions Industry Electronics , vol. 52, no. 5, p.1308–1314, 2005

[3] Covic GA, Boys JT, Kissin MLG, Lu HG. "A three-phase inductive power transfer system for roadway-powered vehicles," IEEE Transactions Industry Electron , vol.54, no. 6, pp.3370–3378,2007

[4] M. A. Razzak, S. Takamura, N. Ohno, Y. Uesugi, "Design of a novel T-LCL immittance conversion circuit for dynamic and non-linear loads," International Conference on Electrical and Computer Engineering, 2006:p.13–16.

[5] M. B. Borage, K. V. Nagesh, M. S. Bhatia, S. Tiwari. "Characteristics and Design of an Asymmetrical Duty-Cycle-Controlled LCL-T Resonant Converter," IEEE Transactions on Power Electronics, 2009,vol.24, no.10, p.2268-2275.

[6] Diecker, S., M.J. Ryan, and R.W. De Doncker. "Design of an IGBT based LCL-resonant inverter for high-frequency induction heating," Conference Record - IAS Annual Meeting (IEEE Industry Applications Society), 1999,p.2039-2045.

[7] H. William, A. P. Hu, S. Akshya. "A wireless power pickup based on directional tuning control of magnetic amplifier," IEEE Transactions on Industrial Electronics, vol.56, no.7, p.2771-2781,2009.

[8] P. Si, A. P. Hu, M. Simon, B. David. "A frequency control method for regulating wireless power to implantable devices," IEEE Transactions on Biomedical Circuits and Systems, 2008, vol.2, no.1, p.22-29,2008

[9] Huang. Shyh-Jier, Lee. Tsong-Shing, Pai. Fu-Sheng, Huang. Tzyy-Haw. "Method of feedback detection for loosely coupled inductive power transfer system with frequency-tracking mechanism,". IEEE 10th International Conference on Power Electronics and Drive Systems (PEDS),2013, p:784-787.

[10] J. T. Boys, G. A. Covic,, Green A. W. "Stability and control of inductively coupled power transfer systems," Electric Power Applications, vol.147, no.1, p.37-43, 2000.

[11] Y. Li, Y. Sun and X. Dai, "Study on multiple resonant points control strategy of contactless power transfer system using neural network," 8th World Congress on Intelligent Control and Automation, 2010, p.1-6.

[12] [Xin Dai, Aiguo Patrick Hu, Chunsen Tang. "Investigating a H∞ Control Method Considering Frequency Uncertainty for CLC Type Inductively Coupled Power Transfer System," IEEE Energy Conversion Congress and Exposition ,2011, p.2022-2027.

[13] T. P Duong, J. Lee, "Experimental results of high-efficiency resonant coupling wireless power transfer using a variable coupling method," IEEE Microw. Wireless Compon. Let., vol. 21, no. 8, p. 442-44, Aug. 2011.